Proceedings of 10th International Conference on Precision, Meso, Micro and Nano Engineering (COPEN 10)
December 07 – 09, 2017, Indian Institute of Technology Madras, Chennai – 600 036 INDIA

Numerical Simulation of Laser Surface Structuring By Remelting of Titanium Alloy

Shashank Sharma[1*], Anup Singh[2], S. A. Ramakrishna[3], J. Ramkumar[1]

[1]Department of Mechanical Engineering, Indian Institute of Technology Kanpur - 208016, INDIA
[2]Department of Mechanical Engineering, Indian Institute of Information Technology, D&M, Jabalpur-482005, INDIA
[3]Department of physics, Indian Institute of Technology Kanpur - 208016, INDIA

Abstract

The surface of a product is profoundly related to its properties and function such as abrasion, corrosion, and scratch resistance which make surface structuring a crucial factor in industries. Laser remelting can be used to generate complex surface structures such as sinusoidal, rotational symmetric wave and helical structures. Moreover, it does not require any surface finishing operation as compared to conventional methods. Surface structuring due to laser remelting is a result of self-organization of molten material under the influence of surface tension and thermal flux driven Marangoni flow, control of which is essential for generating different types of surface structures. To understand its underlying principal and melt pool dynamics, a numerical model is developed which takes into account the processing parameters such as spatial power modulation, scanning speed and peak laser intensity. It has been found out that spatial power modulation and scanning speed affect the surface structure geometry profoundly. The experimental results validate the phenomenon in numerical simulation.

Keywords: Laser remelting, Surface Structuring, Titanium alloy, Modelling and Simulation, Melt pool dynamics.

1. INTRODUCTION

In the recent past, many researchers have shown interest in producing textures or structures of desired geometrical shape on a metallic surface. The texturing or structuring of a surface aims to modify and control essential properties such as wetting properties, optical properties, flow properties and surface adsorption. Further, the surface of any part or product has a significant constraint over its abrasive, scratch resistive, and corrosive properties. Therefore, surface structuring in micro and macro scale are essential in enhancing specific functional performance of the product. In the last decade, there have been numerous attempts by researchers to develop a technique for achieving desired structured on metallic surfaces [1, 2]. Techniques such as mold based patterning using electro-chemical etching or electric discharge machining, conventional machining are used to produce specific geometric structures [2]. Further, lasers with short pulse duration are used to obtain periodic surface structures (laser ablated surface) which are random as far as geometrical aspects are considered.

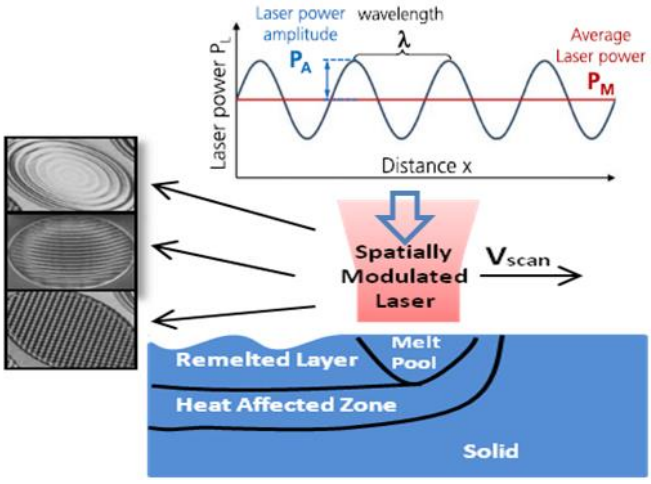

Fig.1 Schematic diagram for Laser remelting [3]

However, the aforementioned methods are based on the principle of subtractive machining. Further these methods require finishing operation in addition making them energy inefficient. In 2015, Temmler et al. [3, 4] developed a new method in which the material irradiated by the laser is melted and reallocated to form structures of definite shapes over a range of metals and metallic alloys. This process is based on the principle of remelting which is quite unlike structuring by laser ablation, resulting in the removal of material. Further, they reported that the resulting structures have low micro roughness. The principle of structuring via remelting is derived from capillary wave excitation and relaxation on the surface of viscous liquid under the influence of temperature dependent surface tension. In other words, when the laser is irradiated on a rough surface due to the effect of surface tension the molten metal flows from a peak of the roughness spikes to its valley, creating a comparatively smooth surface [5]. Therefore to control the resulting surface structure, temperature distribution along the surface can be varied to obtain different flow characteristics under temperature dependent surface tension. Thus, a spatially modulated heat source is projected on to the top surface of the material. Due to absorption of energy from the laser, the temperature of the material rises above the melting temperature and melt pool is formed. After the melt pool is formed, the capillary forces (surface tension and Marangoni convection) become prominent. This along with a spatially changing heat source produce desired geometrical features. Based on the nature of spatial modulation of laser source various kinds of surface structures can be produced which are difficult to produce using conventional machining. Fig. 1 gives a schematic representation of how laser remelting is processed to form different kinds of surface structures.

Therefore, for a better understanding of the melt pool dynamics, there is a need to develop a competent numerical model which can complement the experimental data present in literature. Thus, in this paper, a 2D numerical model of laser structuring is presented which considers phase change, the effect of surface tension, thermo-capillary forces. Further, this model accurately predicts the geometrical changes during melting and solidification of the thin molten layer under the effect of surface tension. The numerical model is validated through experimental data reported by Temmler et al. [4].

ISBN: 978-93-80689-28-9

2. MODEL DESCRIPTION

The model presented in this paper was developed in COMSOL Multiphysics® software for understanding the melt pool dynamics during laser structuring.

A. *Assumptions for Development of Model*

In the present model, in order to demonstrate the effect of surface structuring a sinusoidally modulated heat source (fig. 2) is used, having average power P_M and a spatial wavelength λ with an amplitude P_A. It is pertinent to note here that the spatial beam profile is different from laser power modulation, which is assumed to be a top hat profile in this study. While the power was modulated the laser beam was moved with a constant unidirectional velocity (v) over the surface. For the sake of simplicity melt flow during the single scan will be considered. The range of P_A should be selected such that the maximum temperature attained in the process lies below its vaporization point. Further, in the sinusoidal power modulation, the minimum power level should be sufficient to sustain a melt pool on the surface. During simulation, a sinusoidal spatially modulated laser heat source with its power ranging from 100 - 255 W was applied to the top surface of the material. A spot radius of 250μm was used in the simulation along with a scanning speed of 50mm/s. The laser parameters used in the numerical model are tabulated in table 1. These parameters were selected in accordance with the experimental study done by Temmler et al. [4]. The material of interest for this model is Titanium alloy (Ti-6Al-4V). Its material properties are listed in Table 2 [6, 8].

TABLE 1
Laser Parameters for Simulation

Parameter	Value
Laser spot radius (μm)	250
Ambient temperature (K)	293.15
Average laser power, P_M (W)	177.5
Amplitude of laser power, P_A (W)	77.5
Spatial wavelength, λ (mm)	1
Absorptivity	0.4

For the simulations, melt flow was assumed to be laminar and incompressible Newtonian fluid.

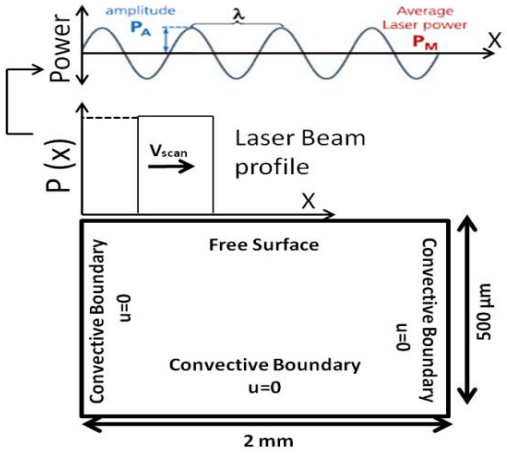

Fig. 2 Schematic diagram of computational domain

Governing Equations

Mass Conservation:

The continuity equation for the phase change in the computational domain is given by

$$\frac{\partial \rho}{\partial t} + \nabla.(\rho \vec{u}) = 0 \quad (1)$$

Energy Conservation:

The governing heat transfer equation during the phase change in the computational domain is given by

$$\frac{\partial(\rho C_P T)}{\partial t} + \vec{u}.\nabla(\rho C_p T) = \nabla.(K \nabla T) \quad (2)$$

During phase change, the values of ρ, Cp and k were determined by the following equations

$$\rho = \theta \rho_{phase\ 1} + (1-\theta)\rho_{phase\ 2} \quad (3)$$

$$C_p = \frac{1}{\rho}\left(\theta \rho_{phase1} C_{p,1} + (1-\theta)\rho_{phase2} C_{p,2}\right) + L\frac{\partial \alpha_m}{\partial T} \quad (4)$$

$$k = \theta k_{phase\ 1} + (1-\theta) k_{phase\ 2} \quad (5)$$

In eq. (3-5) phase1 represents the solid phase i.e., solid metal, phase2 represents the liquid phase i.e., molten metal, θ is a linear function, varying between 1 and 0 and representing the fraction of phase before the transition.

Momentum Conservation:

The governing momentum conservation equation is given by

$$\frac{\partial(\rho \vec{u})}{\partial t} + \vec{u}.\nabla(\rho \vec{u}) = -\nabla p + \nabla.(\mu(\nabla \vec{u} + (\nabla \vec{u})^T) + \vec{F} \quad (6)$$

This equation is implemented in the whole computational domain including melted and solid metal region. For dissipating velocity field in the solid region, the viscosity is assigned a very high value (~108) in that phase.

Natural Convection:

The buoyant flow is included in this model with the help of Boussinesq approximation. The source term $\vec{F}$ in Eq. (6) is given as

$$\vec{F} = \rho_{liquid} \vec{g} \beta_T (T - T_{ref}) \quad (7)$$

In eq. 7, ρliquid, βT and Tref are the density of the liquid, the coefficient of thermal expansion and the reference temperature, respectively.

Marangoni Convection:

The following equation describes the forces that the Marangoni convection [7] induces on the interface at the free surface

$$\mu\left(\frac{\partial u}{\partial y}\right) = -\left(\frac{\partial \gamma}{\partial T}\right)\left(\frac{\partial T}{\partial x}\right) \quad (8)$$

In eq. (8) μ and γ are viscosity and surface tension, respectively.

D. *Boundary Conditions*

The heat energy from the modulated laser heat source is approximated by the formula given by

$$q = A\left(P_M + P_A \sin\frac{2\pi}{\lambda}x\right)/\pi D_L^2 \quad (9)$$

Where A is absorptivity of Titanium alloy. Energy balance at the top surface leads to the following boundary equation

$$k\frac{\partial T}{\partial n} = q - h_c(T - T_\infty) - \varepsilon\sigma\left(T^4 - T_\infty{}^4\right) \quad (10)$$

In Eq. 10 terms on the right-hand side are heat energy from the laser beam, convective heat loss and radiation heat loss to the surrounding, respectively. In Eq. (10) h_c is the convective heat transfer coefficient, ε is the emissivity and σ is the Stefan-Boltzmann constant.

Force balance at the top surface leads to the following boundary equation.

$$\left[\mu\left(\vec{\nabla u} + \left(\vec{\nabla u}\right)^{\mathrm{T}}\right)\right]\vec{n} = \sigma k\nabla\varphi\vec{\imath} + \frac{\partial\sigma}{\partial \mathrm{T}}\frac{\partial \mathrm{T}}{\partial \mathrm{x}}\vec{\jmath} \quad (11)$$

Above boundary condition mainly describes the dynamics of surfaces structuring. The first term contributes towards the effect of surface tension i.e. minimizing energy distribution by changing the shape of its surface whereas the second term accounts for Marangoni convection (Eqn. 8) which is responsible for distribution of molten metal according to the distribution of temperature in the domain.

As for rest of three boundaries, heat flux balance at rest of the surfaces leads to the following boundary equation

$$-K\nabla T = -h_c\left(T - T_{ref}\right) \quad (12)$$

No slip at the rest of the surfaces leads to o the following boundary equation

$$u = 0 \quad (13)$$

To accurately predict the surface profile during laser structuring process, an Arbitrary Lagrangian-Eulerian moving mesh is used. The mesh velocity depends on the velocity field obtained by solving the momentum equation (Eq. 6).

3. RESULTS AND DISCUSSION

Fig.ure 3 illustrates the evolution of peak temperature with time. It is interesting to note that the peak temperature in the melted region oscillates sinusoidally within the range 2000K-2800K, this can be attributed to the fact that when a sinusoidal heat source moves uni-directionally along a surface there will be regions exposed with radiation having power (P_M+P_A) leading to temperature peaks in fig. 3, whereas there will be some region where the cumulative power will be (P_M-P_A) resulting in the temperature valleys in fig. 3. Further, the first minimum of peak temperature occurs at 20ms, with scanning velocity of 50 mm/s the total distance traveled during this time interval is 1 mm which is also the spatial wavelength (λ) of the modulated heat source. Therefore, from fig. 3 it can be concluded that the modulation of heat source will result in a spatial and temporal variation of surface temperature having the same spatial wavelength as that of the heat source.

Fig. 4 depicts the variation of melt pool width and depth with time. The melt pool width varies from 290 μm to 550 μm, and the variation in depth is from 8 μm to 155 μm. The sinusoidal oscillation of melt pool dimensions matches with a variation of peak temperature, which is rather intuitive. However, it is important to note that in fig. 5, within the spatial wavelength (λ= 1mm) contraction of melt pool volume occurs as it progresses with time. For instance at the normalized distance X'=0 (x=-2 mm in the computational domain), at 8 ms the temperature is at its peak resulting in an increase in melt pool volume. When the laser beam progresses due to its spatial modulation (λ) the temperature decreases at (X'~0.8 mm) resulting in a shallow melt volume. Fig. 6, depicts the temperature distribution and convection pattern in the melt pool at 48 ms. There is a shallow depression in the middle, as the melt flow is radially outward from the center.

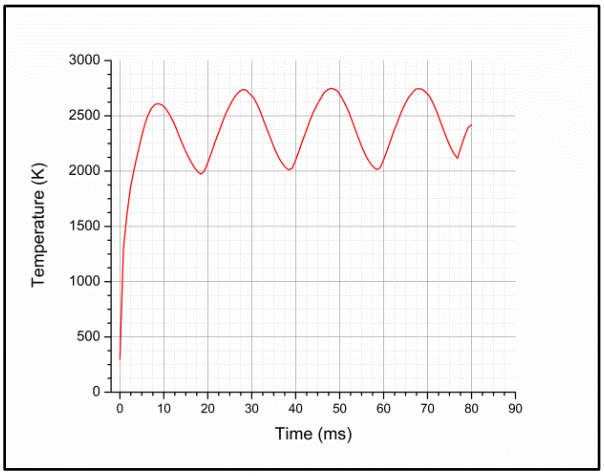

Fig.3 Evolution of peak temperature with time

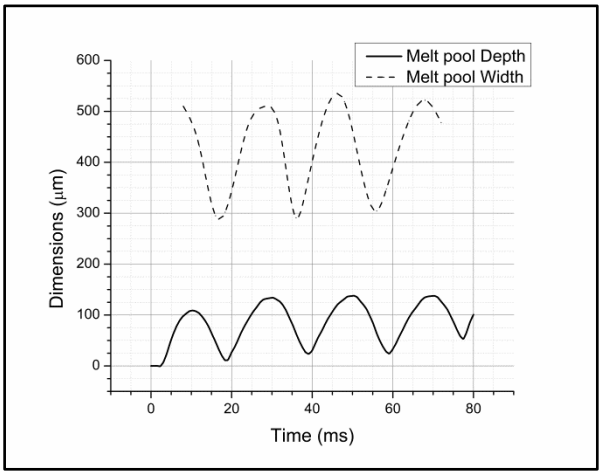

Fig. 4 Evolution of melt depth with time

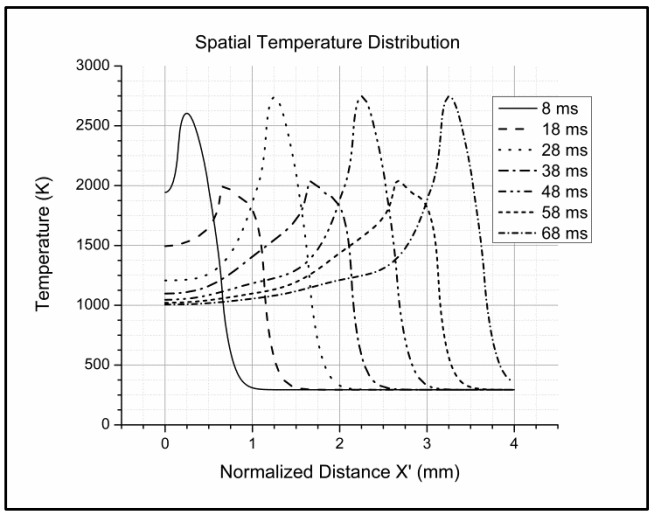

Fig. 5 Spatial Temperature distribution with time

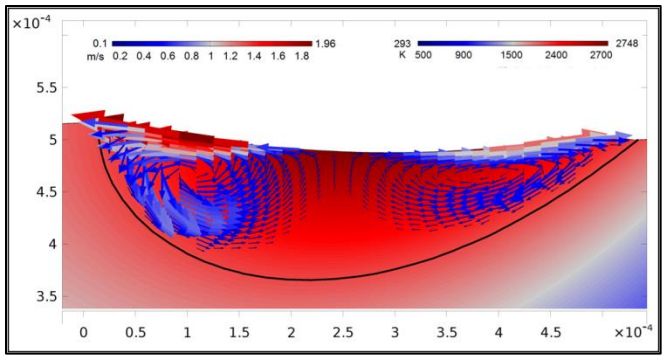

Fig. 6 Temperature and velocity field in melt pool at 48 ms.

The radially outward flow can be attributed to the temperature dependence of surface tension of molten titanium. As melting progresses temperature at the center of the melt pool increases (see fig. 5) which in turn decreases the surface tension. Therefore, the flow occurs from low surface tension region towards the periphery of the melt pool where surface tension is more. It is pertinent to note that with radially outward flow melt deposition occurs near the periphery of melt pool. Fig. 6 shows the evolution of surface structures as the melt pool propagates along the surface, clearly depicting the formation of a sinusoidally structured surface. It should be noted that there are two primary mechanisms that have significance over structure formation, firstly the radially outward flow which deposits the molten metal near the periphery and secondly the variation in the volume of melt pool owing to non uniform temperature distribution on the irradiated surface. As the laser power varies according to its spatial wavelength "λ". The volume of the melt pool will first increase which augments the melt deposition near the receding edge of the melt pool. This melt deposition phenomenon will create a bulged surface towards the end of the progressing melt pool. Once the laser propagates further, the molten material solidifies following the bulged surface. Due to the sinusoidal modulation, the laser power will now decrease thus reducing the melt volume with each time step. Because of low melt volume, the Marangoni convection in this region will also start to diminish creating a shallow melted region adjacent to the solidified bulge. Thus a structured surface having one peak followed by a shallow valley will be produced. The same mechanism will be extended over the complete scan length and the number of peaks will depend upon the spatial wavelength of laser power.

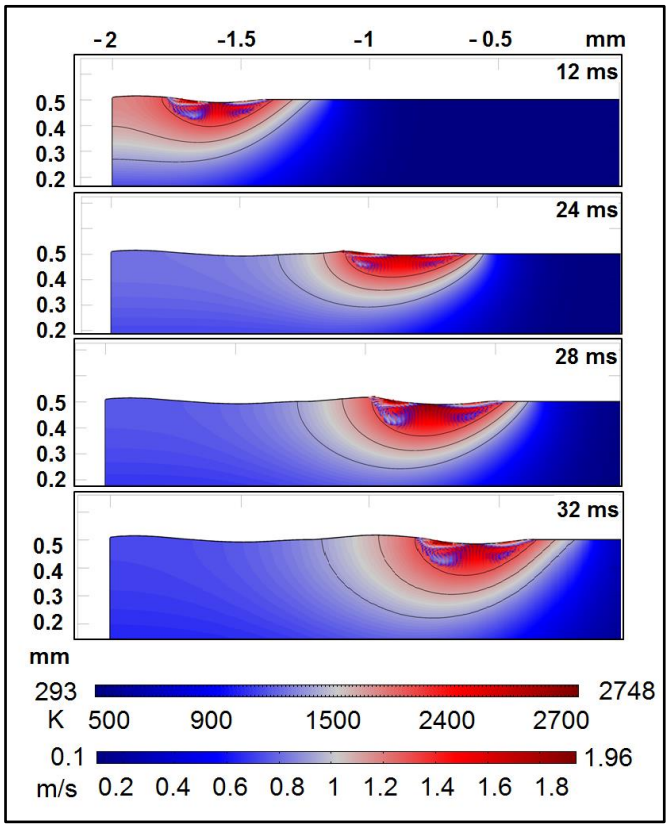

Fig. 7 Evolution surface structure with the progression of melt pool along the irradiated surface.

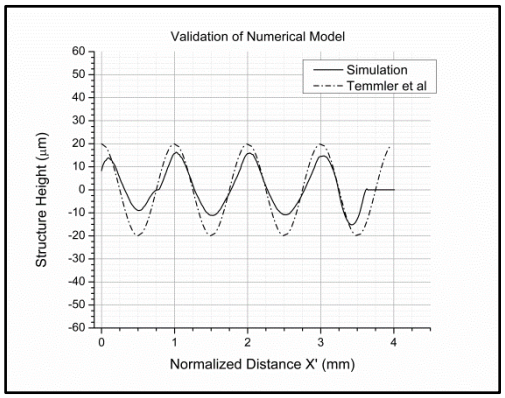

Fig. 7 Two-dimensional profile comparison between experimental and simulation

Fig. 7 depicts the final profile generated after laser structuring by remelting the substrate. The maximum peak to valley height is 30 µm. In fig. 7 results reported by Temmler et al. [4] is also plotted alongside the simulated profile. The difference in amplitude of simulated and experimental profile is not more than 10 µm. The small percentage of error between simulated and experimental data may arise due to the discrepancy in material properties which are based on published results and empirical data.

TABLE 2
Thermophysical properties of Ti-6Al-4V

Melting Temperature (K)	1923
Vaporization Temperature (K)	3533
Solid specific heat (J kg^{-1} K^{-1})	483.04 + 0.215T T ≤ 1268 412.7 + 0.1801T 1268 < T ≤1923
Liquid specific heat (J kg^{-1} K^{-1})	831
Thermal conductivity (W m^{-1} K^{-1})	1.25 + 0.015T T ≤ 1268 3.15 + 0.012T 1268 < T ≤ 1923 -12.75 + 0.024T T>1923
Solid density (kg m^{-3})	4420 – 0.154 (T – 298)
Liquid density (kg m^{-3})	4122
Latent heat of fusion (kJ K^{-1})	286
Latent heat of vaporization (kJK^{-1})	9830
Dynamic viscosity (N m^{-1} s^{-1})	3×10^{-3}
Thermal expansion coefficient (K^{-1})	1.1×10^{5}
Surface tension coefficient (N m^{-1} K^{-1})	-0.28×10^{-3}

4. CONCLUSION

Surface structuring by laser remelting using a spatially modulated power distribution is a new approach for performing structuring of metallic surfaces. To examine the relevance of melt pool in the surface structuring numerical simulation is carried out followed by comparison with experimental data. The model shows good agreement with experimental results. In the numerical study, it has been observed that the melt pool dimensions have direct dependency towards power modulation resulting in non uniform distribution of melt volume along the surface. Further, it has been found out that the radially outward flow due to Marangoni convection is responsible for structuring (bulged surface) the surface. However, the melt pool convection was relevant only in the high power region where the amount of melted volume was sufficient. In conclusion, the structure height is scaled by laser power amplitude and the melt flow due to temperature dependent surface tension. Since the investigations were limited to single scan results, the dependency of structure height with number of scans requires further appraisal.

References

[1] Coblas, Daniela G., et al. "Manufacturing textured surfaces: State of art and recent developments." Proceedings of the Institution of Mechanical Engineers, Part J: Journal of Engineering Tribology 229.1 (2015): 3-29.

[2] Patel, Divyansh, V. K. Jain, and J. Ramkumar. "Micro texturing on metallic surfaces: State of the art." Proceedings of the Institution of Mechanical Engineers, Part B: Journal of Engineering Manufacture (2016): 0954405416661583.

[3] Temmler, André, Edgar Willenborg, and Konrad Wissenbach. "Design surfaces by laser remelting." Physics Procedia 12 (2011): 419-430.

[4] Temmler, A., et al. "Surface structuring by remelting of titanium alloy Ti6Al4V." Journal of Laser Applications 27.S2 (2015): S29103.

[5] Tokarev, V. N., and V. I. Konov. "Suppression of thermocapillary waves in laser melting of metals and semiconductors." Journal of applied physics 76.2 (1994): 800-805.

[6] Rai, R., et al. "Heat transfer and fluid flow during electron beam welding of 21Cr–6Ni–9Mn steel and Ti–6Al–4V alloy." Journal of Physics D: Applied Physics 42.2 (2008): 025503.

[7] Lei, Y. P., et al. "Numerical analysis of the competitive influence of Marangoni flow and evaporation on heat surface temperature and molten pool shape in laser surface remelting." Computational Materials Science 21.3 (2001): 276-290.

[8] Sharma, Shashank, et al. "A study on hydrodynamics of melt expulsion in pulsed Nd: YAG laser drilling of titanium." Proceedings of the 2015 COMSOL Conference, Pune 29–30 October 2015. 2015.